

Will the Up and Down Quarks Always Spin Opposite in the Proton?

Tianbo Liu,^{1,2,*} Raza Sabbir Sufian,¹ Guy F. de T ramond,³
 Hans G nter Dosch,⁴ Stanley J. Brodsky,⁵ and Alexandre Deur¹
 (HLFHS Collaboration)

¹Thomas Jefferson National Accelerator Facility, Newport News, VA 23606, USA

²Department of Physics, Duke University, Durham, NC 27708, USA

³Laboratorio de F sica Te rica y Computacional, Universidad de Costa Rica, 11501 San Jos , Costa Rica

⁴Institut f r Theoretische Physik der Universit t, D-69120 Heidelberg, Germany

⁵SLAC National Accelerator Laboratory, Stanford University, Stanford, CA 94309, USA

We utilize a new approach to hadron dynamics and spectroscopy based on gauge/gravity correspondence, light-front holography, and Veneziano duality to predict the spin-dependent quark distributions of the nucleons. The polarized quark distributions are uniquely determined in terms of the unpolarized distributions without the introduction of additional free parameters. The predictions are consistent with existing experimental data and agree with perturbative QCD constraints at large x . In particular, we predict the sign reversal of the polarized down-quark distribution in the proton at $x \sim 0.8$, a key property of nucleon substructure which will be tested very soon in upcoming experiments.

Introduction.—Understanding how the spin of the proton originates from its quark and gluon constituents is one of the most active research frontiers in hadron physics [1, 2]. A key challenge is to determine the polarized parton distribution functions (PDFs), $\Delta q(x, Q)$, which describe the difference of the probability density between helicity-parallel and helicity-antiparallel quarks in a proton. Here x is the light-front longitudinal momentum fraction of the proton carried by quarks of flavor q . The PDFs represent the universal frame-independent distribution functions of the proton which are measured in deep inelastic lepton-proton scattering (DIS) at space-like momentum transfer Q . Since they are determined by fundamental dynamics of color confinement, they are nonperturbative quantities. It is thus challenging to derive the quark distributions from first principles. However, the x -dependence at large x and the magnitude of the PDFs in the $x \rightarrow 1$ limit are constrained by perturbative QCD (pQCD) [3, 4]. These important constraints [3, 5], which are first-principle predictions of pQCD, predict the helicity retention at $x \sim 1$; *i.e.*, the helicity of a quark carrying large momentum fraction will tend to match the helicity of its parent nucleon: the helicity asymmetry $\Delta q(x, Q)/q(x, Q)$ is predicted to approach 1 as $x \rightarrow 1$, where $q(x, Q)$ being the unpolarized PDF.

Precise measurements of $\Delta q(x, Q)$ from polarized lepton-proton DIS are now available [1, 2]. Although the expected increase of $\Delta u/u$ toward 1 as $x \rightarrow 1$ is observed, $\Delta d/d$ is surprisingly found to *remain negative* in the experimentally covered region of $x \lesssim 0.6$ [6–12], without any indication of a sign reversal at large x -value. Global pQCD analyses of the experimental data extrapolated to large x also favor negative values of $\Delta d/d$ at $x \sim 1$ [13–17], as do Dyson-Schwinger equation calculations [18]. This contradiction with the pQCD constraint at $x \rightarrow 1$ challenges our confidence in understanding the large- x behavior of the polarized PDFs.

In this letter, we present a novel approach to polarized quark distributions based on light-front holographic QCD (LFHQCD) [19] and the Veneziano duality [20] to calculate $\Delta q(x)$. This approach provides for the first time a unique determination of the polarized quark distributions with unpolarized quark distributions from nonperturbative color-confining dynamics. Our determination of $\Delta q(x)$ provides an accurate description of the available experimental data and agrees with the pQCD constraints in the $x \rightarrow 1$ limit. In particular, the value of x for the sign reversal of $\Delta d(x)/d(x)$ is predicted, a key prediction which will be tested in upcoming experiments [21, 22].

LFHQCD predicts hadron structure and spectroscopy by embedding light-front dynamics in a higher dimensional gravity theory [23, 24]. This approach to color confinement provides effective semiclassical QCD bound-state equations [24–27], where the confinement potential is determined by an underlying superconformal algebraic structure [28–30]. This unified framework to hadron spectroscopy and structure, which captures essential aspects of the strong interactions, has been utilized to calculate hadron masses and form factors [19]. Because of the increasing interest in parton distributions, LFHQCD-based models have been developed with modifications of the light-front wave functions [31–49]. These phenomenological extensions usually require a large number of parameters to accurately describe PDFs, thereby reducing their predictive power.

Recently, we introduced a new approach for deriving PDFs as well as generalized parton distributions (GPDs) from LFHQCD [50]. It incorporates both Regge behavior at small- x and inclusive counting rules at large- x . This approach can simultaneously produce the nucleon and pion unpolarized PDFs with minimal parameters, keeping the predictive power with the universality of the reparametrization function. Motivated by these successes, we will extend the formalism here to polarized

distributions; no additional parameters will be required.

Formalism.—We first briefly review the derivation of unpolarized proton PDFs from the holographic expression of its spin-non-flip Dirac form factor $F_1(t)$, where $t = -Q^2$ is the square of transferred momentum. The contribution from a twist- τ Fock state in the light-front Fock expansion of the proton eigensolution, a component with effectively τ constituents, to the Dirac form factor is given by [19, 51]

$$F_1(t) = c_{V,\tau} F_{V,\tau}(t) + c_{V,\tau+1} F_{V,\tau+1}(t), \quad (1)$$

with

$$F_{V,\tau}(t) = \frac{1}{N_{V,\tau}} B\left(\tau - 1, \frac{1}{2} - \frac{t}{4\lambda}\right). \quad (2)$$

The subscript V indicates the coupling to a vector current. λ is the universal mass scale in LFHQCD, which can be fixed by hadron spectroscopy; the fit to the ρ/ω trajectory gives $\sqrt{\lambda} = 0.534 \text{ GeV}$. The $c_{V,\tau}$ and $c_{V,\tau+1}$ are coefficients to be determined, $N_{V,\tau}$ is a normalization factor, and $B(x, y)$ is the Euler beta function. The two terms in Eq. (1) correspond to the contribution from the two chiral components, Ψ_+ and Ψ_- , of the bulk field solution [19]. Eq. (2) has the same structure as a generalization of the Veneziano amplitude $B(1 - \alpha(s), 1 - \alpha(t))$ [20] to non-strong process [52, 53], here electron-nucleon scattering. This amounts to replace the s -dependence $1 - \alpha(s)$ by a constant, which determines the asymptotic behavior of the form factor for large negative values of t [52, 53]. Our framework thus incorporates nonperturbative analytic structures found in pre-QCD studies, such as Regge trajectories and generalized Veneziano amplitudes.

The t -dependence in Eq. (2) can be rewritten as $1 - \alpha_V(t)$ with the Regge trajectory [50]

$$\alpha_V(t) = \frac{t}{4\lambda} + \frac{1}{2}. \quad (3)$$

This is just the ρ/ω trajectory emerging from LFHQCD for vector mesons with massless quarks [30]. The quark mass correction is negligible for u and d quarks; for the strange quark contribution, the ϕ trajectory shifts the intercept to $\alpha_\phi(0) \approx 0.01$ [54].

The GPDs at zero skewness ξ , obtained from the integral representation of $B(x, y)$, are [50]

$$H_\tau(x, \xi = 0, t) = q_\tau(x) \exp[tf(x)], \quad (4)$$

where the unpolarized PDF $q_\tau(x)$ and the profile function $f(x)$ are related by a universal reparameterization function $w(x)$,

$$q_\tau(x) = \frac{1}{N_{V,\tau}} w(x)^{-\frac{1}{2}} [1 - w(x)]^{\tau-2} w'(x), \quad (5)$$

$$f(x) = \frac{1}{4\lambda} \log\left(\frac{1}{w(x)}\right). \quad (6)$$

The function $w(x)$ obeys the boundary conditions:

$$w(0) = 0, \quad w(1) = 1, \quad w'(x) > 0, \quad (7)$$

$$w'(1) = 0, \quad w''(1) \neq 0. \quad (8)$$

Then for a twist- τ state, the unpolarized PDF is

$$q(x) = c_{V,\tau} q_\tau(x) + c_{V,\tau+1} q_{\tau+1}(x). \quad (9)$$

Now, we turn to the polarized distributions, for which the coupling of an axial current – rather than a vector current – is needed. Since the current operator differs by a γ_5 , the axial form factor follows Eq. (1), but with a sign flip from the contribution of the chiral-odd component,

$$F_A(t) = c_{A,\tau} F_{A,\tau}(t) - c_{A,\tau+1} F_{A,\tau+1}(t), \quad (10)$$

where

$$F_{A,\tau}(t) = \frac{1}{N_{A,\tau}} B\left(\tau - 1, 1 - \frac{t}{4\lambda}\right), \quad (11)$$

where the subscript A indicates the coupling to an axial current. $F_{A,\tau}(t)$ has the same structure as $F_{V,\tau}(t)$, but with the Regge trajectory replaced by the axial one:

$$\alpha_A(t) = \frac{t}{4\lambda}, \quad (12)$$

emerging from LFHQCD [30]. The coefficients in (10) and those in (1) are related since they correspond to the same state. Thus apart from the sign-flip in the second term in (10), they have the same value relative to the normalization factors as given by

$$\frac{c_{V,\tau}}{N_{V,\tau}} = \frac{c_{A,\tau}}{N_{A,\tau}}. \quad (13)$$

Since the normalization convention is arbitrary, we set $N_{V,\tau} = N_{A,\tau} = N_\tau$, and therefore identify the coefficients as $c_{V,\tau} = c_{A,\tau} = c_\tau$ [55].

Following the same procedure, we express the $\Delta q(x)$ for a twist- τ state as

$$\Delta q(x) = c_\tau \Delta q_\tau(x) - c_{\tau+1} \Delta q_{\tau+1}(x), \quad (14)$$

where

$$\Delta q_\tau(x) = \frac{1}{N_\tau} [1 - w(x)]^{\tau-2} w'(x). \quad (15)$$

At large- x , we expand $w(x)$ near $x = 1$ according to the boundary conditions (7) and (8),

$$w(x) = 1 + \frac{1}{2} w''(1) (1 - x)^2 + \mathcal{O}((1 - x)^3), \quad (16)$$

and find that $q_\tau(x)$ and $\Delta q_\tau(x)$ have the same behavior,

$$q_\tau(x) = \Delta q_\tau(x) = \frac{[-w''(1)]^{\tau-1}}{2^{\tau-2} N_\tau} (1 - x)^{2\tau-3} + \dots, \quad (17)$$

where higher powers of $(1-x)$ are suppressed. For both the $q(x)$ (9) and the $\Delta q(x)$ (14), the function is dominated by the first term at large- x , unless its coefficient c_τ vanishes. Then the helicity asymmetry at $x \rightarrow 1$ is

$$\lim_{x \rightarrow 1} \frac{\Delta q(x)}{q(x)} = 1, \quad (18)$$

consistent with the pQCD constraint [3, 5].

The spin-aligned and spin-antialigned distributions are linear combinations of the unpolarized and polarized distributions:

$$q_\uparrow(x) = \frac{1}{2}[q(x) + \Delta q(x)], \quad (19)$$

$$q_\downarrow(x) = \frac{1}{2}[q(x) - \Delta q(x)]. \quad (20)$$

We find, in the large- x limit,

$$q_\uparrow(x) \rightarrow c_\tau q_\tau(x), \quad (21)$$

$$q_\downarrow(x) \rightarrow c_{\tau+1} q_{\tau+1}(x). \quad (22)$$

The two helicity distributions tend respectively to a pure contribution from a single chiral component, Ψ_+ or Ψ_- , of the bulk field solution. Eqs. (21) and (22) provide the asymptotic normalization, which can be used to derive the same relation as in Eq. (13).

From Eq. (17), $q_\uparrow(x)$ and $q_\downarrow(x)$ decrease as $(1-x)^{2\tau-3}$ and $(1-x)^{2\tau-1}$, respectively. For the valence state $\tau = 3$, they behave as $(1-x)^3$ and $(1-x)^5$, consistent with pQCD up to logarithmic corrections [3, 4].

At small- x , $w(x)$ has the linear x -dependence: $w(x) \sim x$. Thus $\Delta q(x)$ decreases faster than $q(x)$ with decreasing x , and the helicity asymmetry behaves as

$$\frac{\Delta q(x)}{q(x)} \sim x^{\frac{1}{2}}, \quad (23)$$

where the exponent $1/2$ is given by the difference between the intercepts of the vector and axial Regge trajectories (3) and (12); the intercepts are shifted by negligible amount when u and d quarks mass corrections are included. When $x \rightarrow 0$, the helicity asymmetry goes to zero,

$$\lim_{x \rightarrow 0} \frac{\Delta q(x)}{q(x)} = 0, \quad (24)$$

which indicates that the helicity correlation between a quark and its parent nucleon disappears. This result is a natural expectation [3], because the constituents and the nucleon have infinite relative rapidity for $x \sim 0$. This property is confirmed by the experimental data [56].

Numerical results.—Up to now, all results have been derived for arbitrary twist- τ components without any specific choices for the coefficients c_τ or for $w(x)$, as long as the general boundary conditions are fulfilled. In order to obtain quantitative predictions for the polarized

distributions, the c_τ values of the c_τ are required. We will determine them via the proton's Dirac form factor. If only valence states are considered, we can express the Dirac form factors of u and d quarks as

$$F_1^u(t) = c_{3,u} F_{V,3}(t) + (2 - c_{3,u}) F_{V,4}(t), \quad (25)$$

$$F_1^d(t) = c_{3,d} F_{V,3}(t) + (1 - c_{3,d}) F_{V,4}(t), \quad (26)$$

where the quark number sum rule has been applied, with $N_\tau = B(\tau - 1, 1/2)$ normalizing $F_{V,\tau}(0)$ to 1. The sea quark constituents, beyond the valence state, are encoded in higher Fock states with additional quark-antiquark pairs. In this work, we will truncate the Fock expansion of the nucleon state up to only one quark-antiquark pair, which is a twist-5 state. As a simplifying procedure to include the sea quark contributions we can add to Eq. (25) and Eq. (26) the terms

$$c_{5,u/d} F_{V,5}(t) - c_{5,u/d} F_{V,6}(t), \quad (27)$$

which assumes that the quark number sum rule is saturated by the contribution from the valence quarks. One can also include the intrinsic strange contribution as in Ref. [54]. We will compare the three situations: i) only the valence state contribution; ii) including the contribution from the $u\bar{u}$ and $d\bar{d}$ pairs; iii) also including the contribution from the intrinsic strange sea, taking results from our previous work [54]. We fix the coefficients by matching to the Dirac form factor [57], as listed in Table I.

TABLE I. Coefficient values fixed by matching to the recent electromagnetic form factor extraction of Ref. [57]. The parameter a in Eq. (31) is fixed by the first moment of the unpolarized valence quark distributions for each case. The last column $g_{A,\min}$ is the isovector axial charge with minimal sea. The meaning of the labels is explained in the text.

Label	$c_{3,u}$	$c_{3,d}$	$c_{5,u}$	$c_{5,d}$	a	$g_{A,\min}$
I	1.782	0.066	—	—	0.407	0.867
II	1.793	0.062	-0.559	-0.516	0.480	0.879
III	1.794	0.060	-0.492	-0.447	0.471	0.881

Since the electromagnetic form factors only measure the difference between quark and antiquark contributions, namely $c_{\tau,u} \equiv u_\tau - \bar{u}_\tau$ and similarly for the d quark, contributions to u_τ and \bar{u}_τ cannot be uniquely separated. However, a lower boundary can be derived from the positivity bounds $q_\uparrow(x) \geq 0$ and $q_\downarrow(x) \geq 0$. With the asymptotic relations (21) and (22), this requirement is fulfilled by the minimal sea contribution,

$$\bar{u}(x)_{\min} = c_{5,u} q_{\tau=6}(x) \quad \text{if } c_{5,u} \geq 0, \quad (28)$$

$$\bar{u}(x)_{\min} = -c_{5,u} q_{\tau=5}(x) \quad \text{if } c_{5,u} < 0, \quad (29)$$

and similarly for \bar{d} . This constraint is stronger than that utilized in Ref. [54], where only the sum $q_\uparrow(x) + q_\downarrow(x) \geq 0$ is required.

Since the sea quark distributions are not separately constrained by electromagnetic form factors, one needs other physical observables that are sensitive to the quark and antiquark contributions individually to determine them separately. Instead of attempting a full separation, which is beyond the purpose of this work, we use the relation of the isovector axial charge,

$$g_A = (\Delta u + \Delta \bar{u}) - (\Delta d + \Delta \bar{d}), \quad (30)$$

to constrain the non-minimal sea quark.

The value of the isovector axial charge $g_A = 1.2732(23)$ is precisely determined by the neutron weak decay [58]. As shown in Table I, its value evaluated with a minimal sea component, $g_{A,\text{min}}$, is smaller than the experimental value. To obtain the value of g_A with the minimal shift $u_\tau \rightarrow u_\tau + \delta_{\tau,u}$, $\bar{u}_\tau \rightarrow \bar{u}_\tau + \delta_{\tau,u}$ and similarly for the d -quark, implies a positive shift $\delta_{\tau=5,u}$ and/or $\delta_{\tau=6,d}$. Therefore, we satisfy the relation (30) by the shift $\delta_{\tau=5,u}$ and $\delta_{\tau=6,d}$, and take the variation between them as part of the theoretical uncertainty.

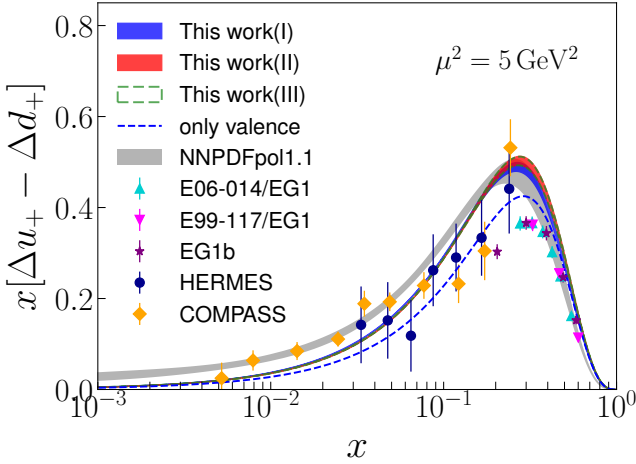


FIG. 1. Polarized distributions of the isovector combination $x[\Delta u_+(x) - \Delta d_+(x)]$ in comparison with NNPDF global fit [15] and experimental data [6–12]. Three sets of parameters, see Table I, are determined from the Dirac form factor and unpolarized valence distributions. The bands represent the variation with different approaches to saturate the axial charge g_A . The blue dashed curve is the valence state contribution without saturating the axial charge.

For the universal reparametrization function $w(x)$, we take the same form as in [50],

$$w(x) = x^{1-x} \exp[-a(1-x)^2], \quad (31)$$

with the parameter “ a ” fixed with the first moment of unpolarized valence quark distributions. One can in principle adopt any parametrization form that fulfills the boundary conditions (7) and (8), and the predictive power is kept by the universality of $w(x)$ for all

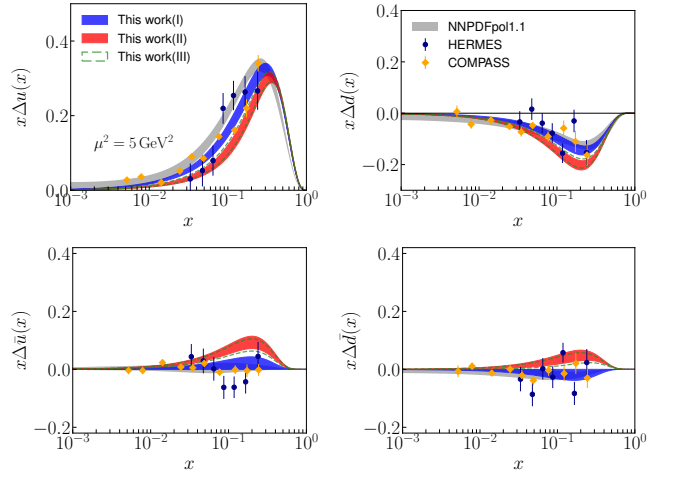


FIG. 2. Polarized distributions of u , d , \bar{u} , and \bar{d} in comparison with NNPDF global fit [15] and experimental data [10–12]. The bands have the same meaning as in Fig. 1.

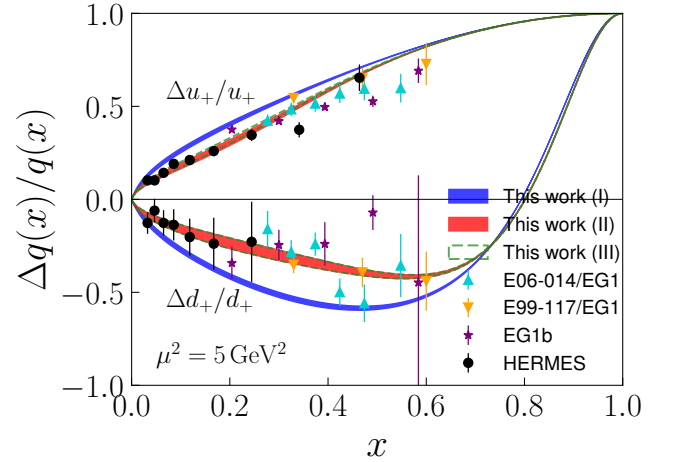


FIG. 3. Helicity asymmetries of $u + \bar{u}$ and $d + \bar{d}$ compared with measurements. The bands and symbols have the same meaning as in Fig. 1.

PDFs. For comparison with measurements, we evolve the PDFs from $Q = 1.06 \text{ GeV}$, which is the matching scale determined from the study of the strong coupling constant [59]. As shown in Figs. 1–3, our numerical results are in good agreement with the global fit [15] and measurements [6–12]. The isovector combination $\Delta u_+ - \Delta d_+$, where u_+ and d_+ stand for $u + \bar{u}$ and $d + \bar{d}$, is the distribution relevant to the relation of the axial charge (30). The dashed blue curve in Fig. 1 is the contribution from the valence state only; the difference with the full results, cases I, II and III, which include saturation of the axial charge is noticeable. This is consistent with the analysis of the Pauli form factor in [60], which demonstrates the significance of the sea quarks in describing spin-related quantities.

As shown in Fig. 2, the variation of our predictions for each flavor from the three sets of coefficients is large, since the sea quark coefficients are not well constrained by the procedure discussed above. Furthermore, the truncation of the Fock state up to five-quark states, which allow only one pair of sea quarks, may potentially result in greater theoretical uncertainties for each individual flavor. The relation Eq. (30) provides an important constraint, but it still leaves some flexibility, such as adding the same term to $u\bar{u}$ and $d\bar{d}$. Since the goal of this letter is to introduce a new approach to the study of polarized PDFs, we will leave this issue to more detailed future investigations.

Most important, the critical region for the upcoming Jefferson Lab spin program [21, 22] is the large- x region, which is dominated by the valence state and is thus much less affected by the variation of the sea. As observed in Fig. 3, the predictions with three sets of coefficients are consistent and very similar in the large- x region. As we have analytically demonstrated above, our approach supports the pQCD prediction that the helicity asymmetry approaches 1 in the large- x limit and follows the power behavior $(1-x)^2$. In particular, the sign-reversal of the d -quark helicity distribution in the proton is robustly predicted to be close to $x \sim 0.8$.

Summary.—We have presented a new approach to the prediction of spin-dependent quark distributions from nonperturbative color-confining dynamics. With all parameters fixed by the nucleon Dirac form factor and unpolarized quark distributions, our predictions for the polarized distributions agree with existing data. Our analytic results for $\Delta q(x)/q(x)$ are consistent with the large- x behavior predicted by pQCD. Our analysis also supports the pQCD prediction of the helicity retention at $x \sim 1$; this fundamental prediction has been challenged by Dyson-Schwinger equation calculations, but it has not yet been constrained by existing data. In the large- x region, where the valence state dominates, we predict that the d -quark helicity will flip its sign at $x \sim 0.8$, regardless of the procedure used to include the sea quark contribution. This prediction will be tested soon [21, 22]. The analytic behavior at large- x and the agreement with existing data reinforces confidence in the pQCD prediction, which can be implemented in global analysis such as that of Ref. [61]. In addition, the relation between the unpolarized and polarized distributions can be tested by simultaneous fits to unpolarized and polarized PDFs.

We would like to thank J.-P. Chen for helpful discussions. This work is supported in part by the U.S. Department of Energy, Office of Science, Office of Nuclear Physics under contracts No. DE-AC05-06OR23177 and No. DE-FG02-03ER41231.

* liutb@jlab.org

- [1] A. Deur, S. J. Brodsky, and G. F. de Téramond, The Spin Structure of the Nucleon, *Rep. Prog. Phys.* **82**, 076201 (2019).
- [2] C. A. Aidala, S. D. Bass, D. Hasch, and G. K. Mallot, The Spin Structure of the Nucleon, *Rev. Mod. Phys.* **85**, 655 (2013).
- [3] S. J. Brodsky, M. Burkardt, and I. Schmidt, Perturbative QCD constraints on the shape of polarized quark and gluon distributions, *Nucl. Phys. B* **441**, 197 (1995).
- [4] H. Avakian, S. J. Brodsky, A. Deur, and F. Yuan, Effect of Orbital Angular Momentum on Valence-Quark Helicity Distributions, *Phys. Rev. Lett.* **99**, 082001 (2007).
- [5] G. R. Farrar and D. R. Jackson, Pion and Nucleon Structure Functions Near $x = 1$, *Phys. Rev. Lett.* **35**, 1416 (1975).
- [6] X. Zheng *et al.* (Jefferson Lab Hall A Collaboration), Precision measurement of the neutron spin asymmetry A_1^N and spin flavor decomposition in the valence quark region, *Phys. Rev. Lett.* **92**, 012004 (2004).
- [7] X. Zheng *et al.* (Jefferson Lab Hall A Collaboration), Precision measurement of the neutron spin asymmetries and spin-dependent structure functions in the valence quark region, *Phys. Rev. C* **70**, 065207 (2004).
- [8] D. S. Parno *et al.* (Jefferson Lab Hall A Collaboration), Precision Measurements of A_1^n in the Deep Inelastic Regime, *Phys. Lett. B* **744**, 309 (2015).
- [9] K. V. Dharmawardane *et al.* (CLAS Collaboration), Measurement of the x - and Q^2 -dependence of the asymmetry A_1 on the nucleon, *Phys. Lett. B* **641**, 11 (2006).
- [10] A. Airapetian *et al.* (HERMES Collaboration), Flavor decomposition of the sea-quark helicity distributions in the nucleon from semiinclusive deep inelastic scattering, *Phys. Rev. Lett.* **92**, 012005 (2004).
- [11] A. Airapetian *et al.* (HERMES Collaboration), Quark helicity distributions in the nucleon for up, down, and strange quarks from semi-inclusive deep-inelastic scattering, *Phys. Rev. D* **71**, 012003 (2005).
- [12] M. G. Alekseev *et al.* (COMPASS Collaboration), Quark helicity distributions from longitudinal spin asymmetries in muon-proton and muon-deuteron scattering, *Phys. Lett. B* **693**, 227 (2010).
- [13] D. de Florian, R. Sassot, M. Stratmann, and W. Vogelsang, Global Analysis of Helicity Parton Densities and Their Uncertainties, *Phys. Rev. Lett.* **101**, 072001 (2008).
- [14] D. de Florian, R. Sassot, M. Stratmann, and W. Vogelsang, Extraction of Spin-Dependent Parton Densities and Their Uncertainties, *Phys. Rev. D* **80**, 034030 (2009).
- [15] E. R. Nocera, R. D. Ball, S. Forte, G. Ridolfi, and J. Rojo, A first unbiased global determination of polarized PDFs and their uncertainties, *Nucl. Phys. B* **887**, 276 (2014).
- [16] P. Jimenez-Delgado, H. Avakian, and W. Melnitchouk, Constraints on spin-dependent parton distributions at large x from global QCD analysis, *Phys. Lett. B* **738**, 263 (2014).
- [17] J. J. Ethier, N. Sato, and W. Melnitchouk, First simultaneous extraction of spin-dependent parton distributions and fragmentation functions from a global QCD analysis, *Phys. Rev. Lett.* **119**, no. 13, 132001 (2017).
- [18] C. D. Roberts, R. J. Holt and S. M. Schmidt, Nucleon spin structure at very high- x , *Phys. Lett. B* **727**, 249 (2013).
- [19] For a review, see *e.g.*, S. J. Brodsky, G. F. de Téramond,

- H. G. Dosch and J. Erlich, Light-front holographic QCD and emerging confinement, *Phys. Rep.* **584**, 1 (2015).
- [20] G. Veneziano, Construction of a crossing - symmetric, Regge behaved amplitude for linearly rising trajectories, *Nuovo Cim. A* **57**, 190 (1968).
- [21] JLab experiment E12-06-110, spokespersons: X. Zheng (contact), G. Cates, J.-P. Chen, and Z.-E. Meziani.
- [22] JLab experiment E12-06-122, spokespersons: B. Wojtsekhowski (contact), J. Annand, T. Averett, G. Cates, N. Liyanage, G. Rosner, and X. Zheng.
- [23] S. J. Brodsky and G. F. de Téramond, Light-front hadron dynamics and AdS/CFT correspondence, *Phys. Lett. B* **582**, 211 (2004).
- [24] S. J. Brodsky, G. F. de Téramond, and H. G. Dosch, Threefold Complementary Approach to Holographic QCD, *Phys. Lett. B* **729**, 3 (2014).
- [25] G. F. de Téramond and S. J. Brodsky, Hadronic spectrum of a holographic dual of QCD, *Phys. Rev. Lett.* **94**, 201601 (2005).
- [26] S. J. Brodsky and G. F. de Téramond, Hadronic spectra and light-front wavefunctions in holographic QCD, *Phys. Rev. Lett.* **96**, 201601 (2006).
- [27] G. F. de Téramond and S. J. Brodsky, Light-Front Holography: A First Approximation to QCD, *Phys. Rev. Lett.* **102**, 081601 (2009).
- [28] G. F. de Téramond, H. G. Dosch, and S. J. Brodsky, Baryon Spectrum from Superconformal Quantum Mechanics and its Light-Front Holographic Embedding, *Phys. Rev. D* **91**, no. 4, 045040 (2015).
- [29] H. G. Dosch, G. F. de Téramond, and S. J. Brodsky, Superconformal Baryon-Meson Symmetry and Light-Front Holographic QCD, *Phys. Rev. D* **91**, no. 8, 085016 (2015).
- [30] S. J. Brodsky, G. F. de Téramond, H. G. Dosch, and C. Lorcé, Universal Effective Hadron Dynamics from Superconformal Algebra, *Phys. Lett. B* **759**, 171 (2016).
- [31] Z. Abidin and C. E. Carlson, Hadronic Momentum Densities in the Transverse Plane, *Phys. Rev. D* **78**, 071502 (2008).
- [32] A. Vega, I. Schmidt, T. Gutsche, and V. E. Lyubovitskij, Generalized parton distributions in AdS/QCD, *Phys. Rev. D* **83**, 036001 (2011).
- [33] A. Vega, I. Schmidt, T. Gutsche, and V. E. Lyubovitskij, Generalized parton distributions in an AdS/QCD hard-wall model, *Phys. Rev. D* **85**, 096004 (2012).
- [34] T. Gutsche, V. E. Lyubovitskij, I. Schmidt, and A. Vega, Light-front quark model consistent with Drell-Yan-West duality and quark counting rules, *Phys. Rev. D* **89**, no. 5, 054033 (2014) [Erratum: *Phys. Rev. D* **92**, no. 1, 019902 (2015)].
- [35] T. Gutsche, V. E. Lyubovitskij, I. Schmidt, and A. Vega, Nucleon structure in a light-front quark model consistent with quark counting rules and data, *Phys. Rev. D* **91**, 054028 (2015).
- [36] D. Chakrabarti and C. Mondal, Generalized Parton Distributions for the Proton in AdS/QCD, *Phys. Rev. D* **88**, no. 7, 073006 (2013).
- [37] D. Chakrabarti and C. Mondal, Chiral-odd generalized parton distributions for proton in a light-front quark-diquark model, *Phys. Rev. D* **92**, no. 7, 074012 (2015).
- [38] M. Dehghani, Hard-gluon Evolution of Nucleon Generalized Parton Distributions in Soft-Wall AdS/QCD Model, *Phys. Rev. D* **91**, no. 7, 076009 (2015).
- [39] D. Chakrabarti, T. Maji, C. Mondal, and A. Mukherjee, Quark Wigner distributions and spin-spin correlations, *Phys. Rev. D* **95**, no. 7, 074028 (2017).
- [40] C. Mondal, N. Kumar, H. Dahiya, and D. Chakrabarti, Charge and longitudinal momentum distributions in transverse coordinate space, *Phys. Rev. D* **94**, no. 7, 074028 (2016).
- [41] T. Maji and D. Chakrabarti, Light front quark-diquark model for the nucleons, *Phys. Rev. D* **94**, no. 9, 094020 (2016).
- [42] T. Maji and D. Chakrabarti, Transverse structure of a proton in a light-front quark-diquark model, *Phys. Rev. D* **95**, no. 7, 074009 (2017).
- [43] M. Traini, M. Rinaldi, S. Scopetta, and V. Vento, The effective cross section for double parton scattering within a holographic AdS/QCD approach, *Phys. Lett. B* **768**, 270 (2017).
- [44] T. Gutsche, V. E. Lyubovitskij, and I. Schmidt, Nucleon parton distributions in a light-front quark model, *Eur. Phys. J. C* **77**, no. 2, 86 (2017).
- [45] T. Maji, C. Mondal, and D. Chakrabarti, Leading twist generalized parton distributions and spin densities in a proton, *Phys. Rev. D* **96**, no. 1, 013006 (2017).
- [46] M. Rinaldi, GPDs at non-zero skewness in ADS/QCD model, *Phys. Lett. B* **771**, 563 (2017).
- [47] A. Bacchetta, S. Cotogno, and B. Pasquini, The transverse structure of the pion in momentum space inspired by the AdS/QCD correspondence, *Phys. Lett. B* **771**, 546 (2017).
- [48] C. Mondal, Helicity-dependent generalized parton distributions for nonzero skewness, *Eur. Phys. J. C* **77**, no. 9, 640 (2017).
- [49] N. Chouika, C. Mezrag, H. Moutarde, and J. Rodríguez-Quintero, Covariant Extension of the GPD overlap representation at low Fock states, *Eur. Phys. J. C* **77**, no. 12, 906 (2017).
- [50] G. F. de Téramond, T. Liu, R. S. Sufian, H. G. Dosch, S. J. Brodsky, and A. Deur, Universality of Generalized Parton Distributions in Light-Front Holographic QCD, *Phys. Rev. Lett.* **120**, no. 18, 182001 (2018).
- [51] S. J. Brodsky and G. F. de Téramond, AdS/CFT and Light-Front QCD, *Subnucl. Ser.* **45**, 139 (2009).
- [52] M. Ademollo and E. Del Giudice, Nonstrong amplitudes in a Veneziano-type model, *Nuovo Cim. A* **63**, 639 (1969).
- [53] P. V. Landshoff and J. C. Polkinghorne, The scaling law for deep inelastic scattering in a new veneziano-like amplitude, *Nucl. Phys. B* **19**, 432 (1970).
- [54] R. S. Sufian, T. Liu, G. F. de Téramond, H. G. Dosch, S. J. Brodsky, A. Deur, M. T. Islam, and B.-Q. Ma, Non-perturbative strange-quark sea from lattice QCD, light-front holography, and meson-baryon fluctuation models, *Phys. Rev. D* **98**, no. 11, 114004 (2018).
- [55] The normalization convention used here corresponds to $\int_0^1 dx q_T(x) = 1$, and $\int_0^1 dx \Delta q_T(x) = \frac{\Gamma(\tau-1/2)}{\sqrt{\pi}\Gamma(\tau)}$.
- [56] E. R. Nocera, Small- and large- x nucleon spin structure from a global QCD analysis of polarized Parton Distribution Functions, *Phys. Lett. B* **742**, 117 (2015).
- [57] Z. Ye, J. Arrington, R. J. Hill, and G. Lee, Proton and Neutron Electromagnetic Form Factors and Uncertainties, *Phys. Lett. B* **777**, 8 (2018).
- [58] M. Tanabashi *et al.* (Particle Data Group), Review of Particle Physics, *Phys. Rev. D* **98**, no. 3, 030001 (2018).
- [59] A. Deur, S. J. Brodsky and G. F. de Téramond, Determination of $\Lambda_{\overline{\text{MS}}}$ at five loops from holographic QCD, *J. Phys. G* **44**, no. 10, 105005 (2017).

- [60] R. S. Sufian, G. F. de T ramond, S. J. Brodsky, A. Deur, and H. G. Dosch, Analysis of nucleon electromagnetic form factors from light-front holographic QCD : The spacelike region, *Phys. Rev. D* **95**, no. 1, 014011 (2017).
- [61] E. Leader, A. V. Sidorov, and D. B. Stamenov, A New evaluation of polarized parton densities in the nucleon, *Eur. Phys. J. C* **23**, 479 (2002).